Iron forbidden lines in tokamak discharges

S. Suckewer and E. Hinnov
Plasma Physics Laboratory, Princeton University, Princeton, New Jersey 08544
(Received 23 February 1979)

Several spectrum lines from forbidden transitions in the ground configurations of highly ionized atoms have been observed in the discharges of Princeton Large Torus tokamak. Such lines allow localized observations, in the high-temperature regions of the plasma, of ion-temperatures, plasma motions, and spatial distributions of ions. Measured absolute intensities of the forbidden lines have been compared with simultaneous observations of the ion resonance lines. Model calculations have been carried out in order to deduce the relative importance of electron collisions and radiative decays in establishing excited-state populations.

I. INTRODUCTION

Recent measurements of ion temperature[1,2] and plasma rotation[3] in the Princeton Large Torus (PLT) tokamak during neutral-beam injection demonstrated the utility of forbidden lines of highly ionized atoms for plasma diagnostics. Ion temperature measurements from Doppler broadening of the forbidden line of Fe XX at 2665.1 Å were performed for a wide range of T_i (0.5 keV $\leq T_i \leq 6.5$ keV). The high potential of ionization ($I_p = 1582$ eV) and strong deviation of ionization states from corona equilibrium provides emission of this line in the central part of the plasma during neutral-beam injection even when the electron temperature reaches $T_e \approx 3-4$ keV. The long wavelength of the Fe XX forbidden line simplified the measurements and improved their accuracy (for example, radial distribution of toroidal plasma rotation was measured during neutral-beam injection into the PLT plasma by using a 0.5-m monochromator in air).

Interest in forbidden lines of highly ionized atoms appeared first in astrophysics[4-6] and only recently also in high-temperature laboratory plasmas.[7-9] In astrophysics, interest in forbidden lines is motivated by the possibility of using them for ion temperature and mass motion, electron temperature, and density measurements in solar flares and in the solar corona.[10-12] Ion temperature and mass motions are based on measurements of line Doppler broadening and shifts, whereas electron temperature and electron density can be deduced from line intensity ratios. The method of line intensity ratio for electron density measurement was developed for laboratory plasmas using Li-like ions.[13] Feldman and Doschek[9,14] extended the method to ratios of highly ionized iron lines (Fe XVIII – Fe XXII) from optically allowed and forbidden transitions. In tokamak plasmas, where a variety of density measurements are available, and measurements with uncertainties in excess of 10%–20% are not of interest, the problem may be reversed in principle, and the measured line intensities and ratios at known electron density may be used to test the adequacy of excitation rates and transition probabilities.

In this paper (Sec. II) we present measurements of forbidden line intensities in the PLT discharges for the three well-identified lines, Fe XVIII 974.8 ± 0.3 Å, Fe XX 2665.1 ± 0.3 Å, and Fe XXII 845.55 ± 0.1 Å. Time evolution and space distribution measurements of the emissivity of these lines and comparison with other highly ionized iron lines form part of the identification process, and are of course also required for localized plasma diagnostics.

In Sec. III we discuss energy levels, configurations, and transitions for Fe XVIII – Fe XXIII forbidden lines observed or expected to be observable in tokamaks. Calculations of the intensity of Fe XVIII 975 Å, Fe XX 2665 Å, and Fe XXII 846 Å lines as a function of electron density are presented and compared with measurements. The effect of radial diffusion of the ions on intensity ratios in tokamak plasmas and the consequent deviation from coronal equilibrium is also discussed.

Finally, Sec. IV presents some concluding remarks on the forbidden lines behavior in tokamak-type plasma and their application for plasma diagnostics.

II. INSTRUMENTATION AND MEASUREMENTS

The measurements of wavelengths, time evolution, and space distribution of emissivities of the forbidden lines of highly ionized iron were carried out in the Princeton Large Torus[15,16] discharges during 1976–78. The discharges are characterized by electron temperatures in the range $T_e = 1.0-2.5$ keV and electron densities $N_e = (3-10) \times 10^{13}$ cm^{-3} in the plasma region where the emission of these lines occurs.

The measurements were performed mainly with

a SPEX 1-m grazing incidence spectrometer, equipped with a 2400/mm holographic grating in spectral range 30–1200 Å, and a 1-m Jarrell-Ash Ebert-Fastie-type monochromator in the range 1200–7000 Å.[17,18] Both instruments were calibrated for absolute intensity measurements. Below 1200 Å radial intensity distributions were obtained by shot-by-shot scanning, whereas above 2000 Å an additional 0.5-m monochromator with a fast rotating mirror was used for single-shot radial scans.[19]

Table I shows the three forbidden lines with wavelengths 845.5, 974.8, and 2665.1 Å which have been observed in PLT and well identified from space and time behavior of their emissivities. The first two of these lines had been observed before in solar flares[20] (with wavelengths reported at 845.1 and 974.8 Å). The third one (2665.1 Å) was first observed[1] in PLT. Two other forbidden lines of C-sequence Fe XXI, at 2304 and 1354.1 Å were also observed in ATC and PLT tokamaks (line 1354.1 Å having been already observed in solar flares[20]), but their wavelengths and intensity distributions were not adequately established (in the near future we hope to perform in PLT definitive measurements for both these lines, when plasma conditions will be appropriate: low oxygen and carbon radiation, relatively high density of iron, $\approx 1-2\times10^{11}$ cm^{-3}, and electron temperature above $T_e > 1.5-2.0$ keV). Table I also shows two predicted forbidden lines, Fe XX and Fe XXIII. These lines will probably be observable in tokamak discharges.

The characteristic appearance times and intensity peak times of the several forbidden lines in typical PLT discharges ($N_e = 3-5\times10^{13}$ cm^{-3}, $T_e = 1.5\times2.0$ keV) are shown in Fig. 1, together with some resonance line behavior of Fe XV and Fe XXIII, Fe XXIV, for comparison. This figure gives an indication of the initial assignment of an observed line to a particular ion species. In all cases there are also simultaneous measurements of the time behavior of the allowed resonance lines of the same ions.

In a typical PLT discharge the peak intensity of the Fe XVIII 975 Å line was 1.1×10^{14} photons cm^{-2} sec^{-1} sr^{-1}, and the ratios I(975 Å)/I(94 Å) $\approx 1/4$, I(975 Å)/I(104 Å) $\approx 1/1.5$. In similar discharge conditions, and with total Fe XX concentration about 7×10^{10} cm^{-3}, the peak intensity of the Fe XX 2665 Å line was 1.2×10^{13} photons cm^{-2} sec^{-1} sr^{-1}. The intensity of the Fe XXII 846 Å at its peak was about 1×10^{14} photons cm^{-2} sec^{-1} sr^{-1} and the ratios of I(846)/I(136) $\approx 1/3$, I(846)/I(156) $= 1/1.6$ and I(846)/I(114) $\approx 1/1.1$. The relative intensities of several other Fe XXII lines related to the 846 Å transition are described in Ref. 26 (see also Fig. 8).

TABLE I. Iron forbidden lines of tokamak interest.

Sequence	Ion	Transition [a] Series	Term	λ(Å) Observation	Predictions [b]	Intensity phonons cm^{-2} sec^{-1} sr^{-1}	A_{nm}(sec^{-1}) [c]	E_n(eV) [d]	IP (eV)
F	Fe XVIII	$2s^22p^5$	$^2P_{1/2}\rightarrow{}^2P_{3/2}$	974.8 ± 0.3 (T, SF)		1.1(+14) [e] (T)	1.9(+4)	12.72	1358
O	Fe XIX	$2s^22p^4$	$^3P_1\rightarrow{}^3P_2$	1118.4 (SF)		···	1.4(+4)	11.08	1456
N	Fe XX	$2s^22p^3$	$^2D_{5/2}\rightarrow{}^2D_{3/2}$	2665.1 ± 0.3 (T)		1.2(+13) (T)	5.7(+2)	20.56	1582
N	Fe XX	$2s^22p^3$	$^2P_{3/2}\rightarrow{}^2P_{1/2}$	···	1585	···	1.6(+3)	38.83	1582
C	Fe XXI	$2s^22p^2$	$^3P_1\rightarrow{}^3P_0$	2300(?) (T)	2304		9.1(+2)	19.14	1689
C	Fe XXI	$2s^22p^2$	$^3P_2\rightarrow{}^3P_1$	1354.1 (SF; T?)			6.8(+3)	14.52	1689
B	Fe XXII	$2s^22p$	$^3P_{3/2}\rightarrow{}^3P_{1/2}$	845.5 ± 0.1 (T, SF)		1.0(+14) (T)	1.5(+4)	14.66	1799
Be	Fe XXIII	$2s2p$	$^3P_2\rightarrow{}^3P_1$	···	1104		9.7(+3)	11.23	1950

[a] References 24 and 25.
[b] Reference 21.
[c] References 22 and 23.
[d] Reference 24.
[e] Read 1.1(+14) = 1.1×10^{14}; T is observation in tokamak (PLT); SF is observation in solar flare (Ref. 20).

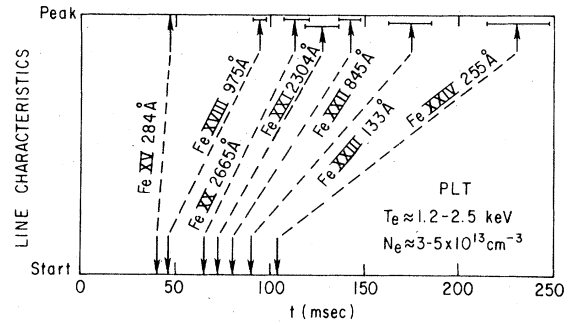

FIG. 1. Time of start and peak intensity of iron Fe XVIII-Fe XXII forbidden lines and Fe XV, Fe XXIII, and Fe XXIV resonance lines in a PLT discharge.

The measurement accuracy of the vacuum uv intensities has been described in Ref. 17, and the actual calibration curves are given in Ref. 37. In the worst case, comparison of the 846 Å with short-wavelength lines, the error may be as large as factor 2, in all other cases probably less than ±30%. In the 2665 Å case, with the spectrometer directly calibrated against a standard lamp, the absolute accuracy is better than ±20%.

III. LEVEL POPULATIONS AND INTENSITY RATIOS

In this section we calculate the populations of the upper levels of the transitions leading to the emission of Fe XVIII 975 Å, Fe XX 2665 Å, and Fe XXII 846 Å lines, and the expected intensity ratios of these lines to the various allowed resonance lines.

The excited level populations are determined predominantly by electron and, in some cases, proton collisional transitions and spontaneous radiative transitions. The line intensities and ratios thus depend directly on the local electron density, and, where proton collisions are important, also on ion temperature. The electron temperature enters only indirectly, determining the radial location of the emitting ions, since the electron energies are typically large compared to transition energies, and the collisional rates hence are only weakly electron-temperature dependent. The density dependence of the forbidden and allowed transitions are generally different, because collisional depopulation rates become competitive with radiative transitions at much lower densities in the case of metastable states.

In tokamak plasmas the radial ion distributions[27] deviate considerably from coronal equilibrium,[28] as shown in a typical case in Fig. 2. This deviation is due to radial motion of the ions, and probably also to charge exchange with neutral hydrogen (which is present in quantities considerably above equilibrium values). Thus calculations or modeling of plasmas that assumes coronal equilibrium distribution of ions can lead to erroneous results. For example, the temperature and density at the ion concentration maxima can be significantly different from values that would correspond to coronal equilibrium.[9,29]

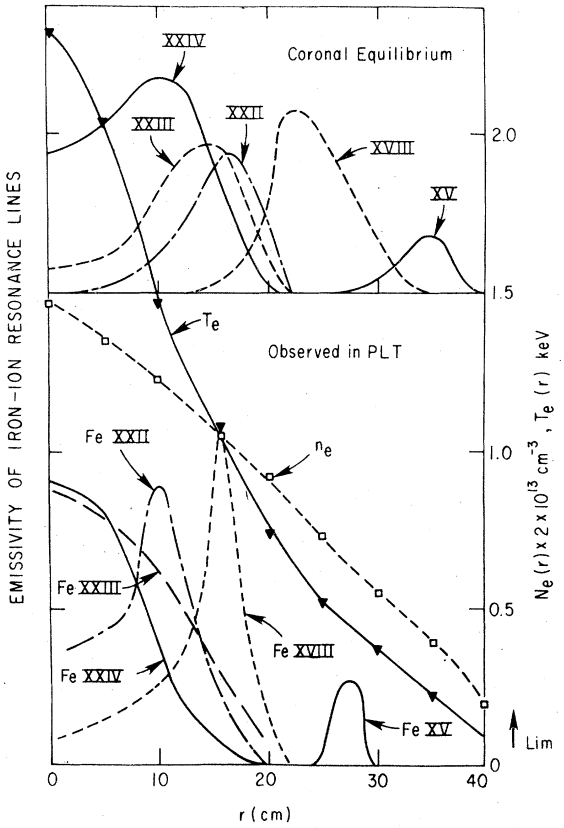

FIG. 2. Observed radial distribution of highly ionized iron lines and the distribution expected in coronal equilibrium, in a PLT discharge.

Calculations of level population as a function of electron density were performed by solving a set of steady-state rate equations in the form

$$\frac{dN_n}{dt} = 0 = -N_n\left(\sum_{m\neq n} A_{nm} + N_e S_{nm} + N_p S^p_{nm}\right) + \sum_{m\neq n} N_m (A_{mn} + N_e S_{mn} + N_p S^p_{mn}) \quad (1)$$

Here A_{nm} is the spontaneous transition probability ($A_{nm} = 0$ if $m \geq n$), S_{mn} is the collisional excitation rate coefficient if $m < n$ or deexcitation coefficient if $m > n$, and the letter "p" indicates protons. From the detailed balance relation we have

$$S_{mn} = S_{nm}\frac{g_n}{g_m}\exp\left(-\frac{E_n - E_m}{kT}\right) \ldots\ldots, \qquad (2)$$

where g_n and g_m are statistical weights, and E_n and E_m are excitation energies of levels n and m from the ground level. As T should be used T_e for electron and T_i for proton excitation and de-excitation collisions. Electron impact excitation rate coefficients of Refs. 30–32 were used while the proton excitation rate coefficients were extrapolated from Bely and Faucher calculations.[33] Coefficients A_{nm} were taken from Refs. 22 and 23. Partial energy level diagrams (Fig. 3) and principal transitions for population of upper levels of the Fe XVIII-Fe XXII forbidden lines were reconstructed from Refs. 24 and 25.

Figure 4 shows the results of calculations of Fe XVIII 975 Å line intensity as a function of electron density N_e together with the intensity from the allowed transitions $2s2p^6\,{}^2S_{1/2} \rightarrow 2s^2 2p^5\,{}^2P_{1/2,3/2}$ (104 and 94 Å), which influence the population of the level $2s^2 2p^5\,{}^2P_{1/2}$ (we will label this level as level 2). Calculations were performed in a three-level scheme. Level 2 was populated directly

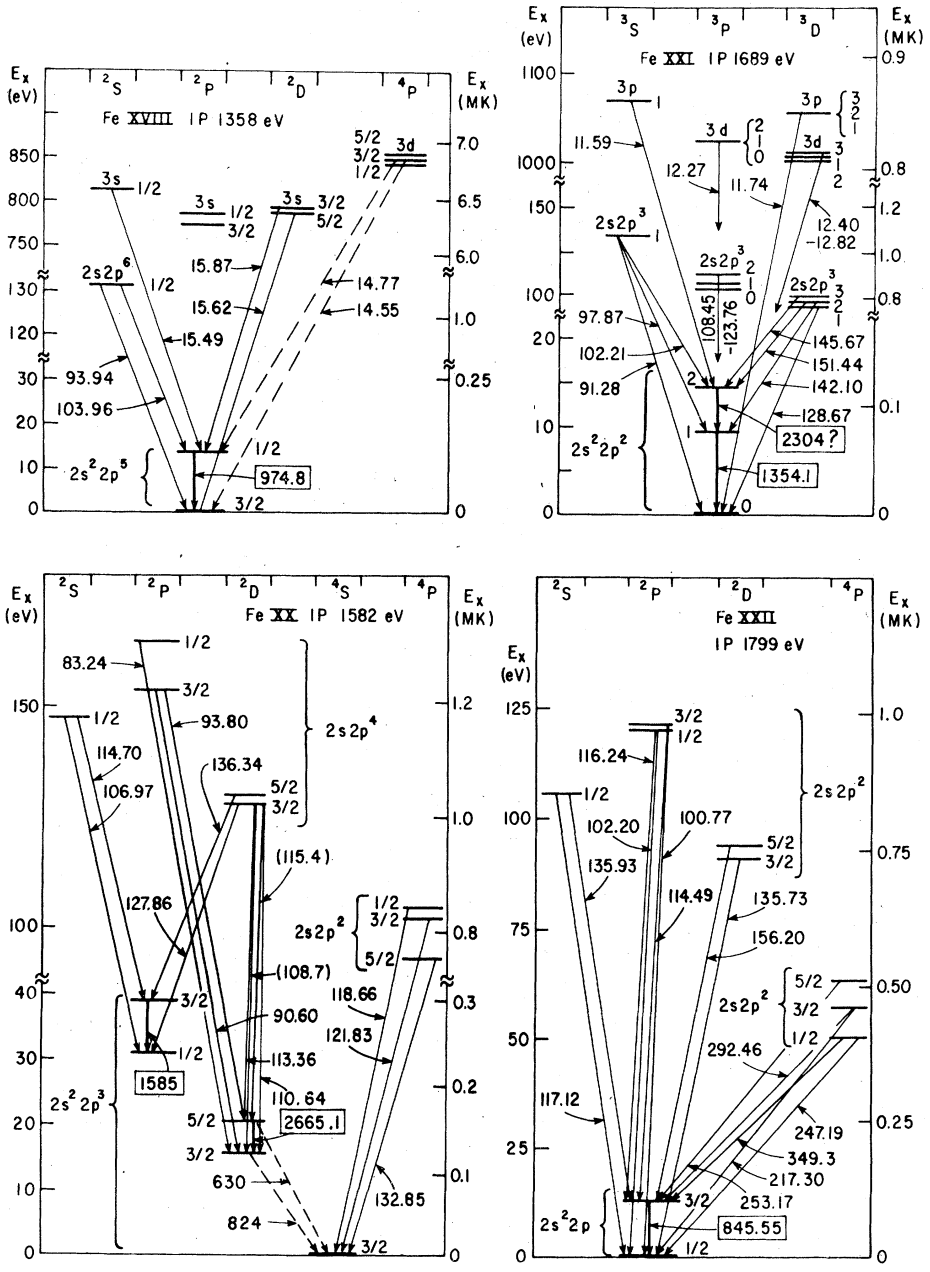

FIG. 3. Partial energy level diagrams for Fe XVIII, Fe XX, Fe XXI, and Fe XXII.

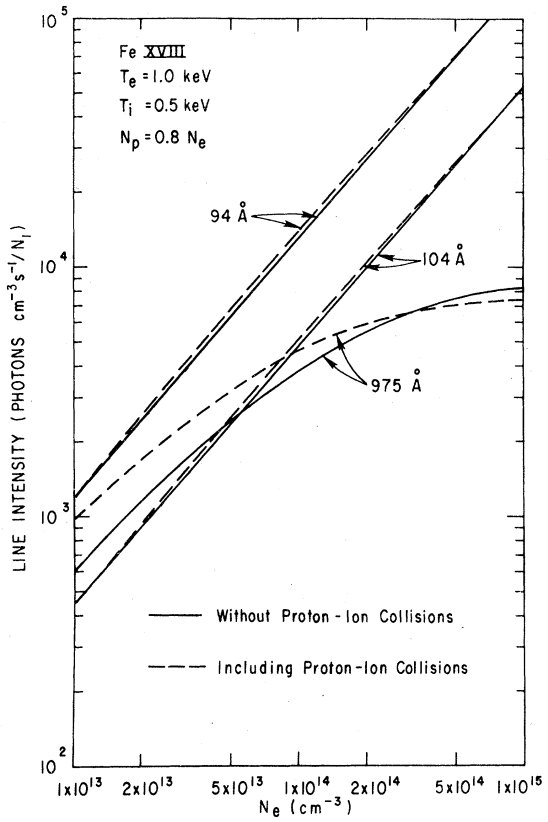

FIG. 4. Calculations of intensities of selected Fe XVIII lines vs electron density. Dashed curves include transitions induced by proton-iron collisions.

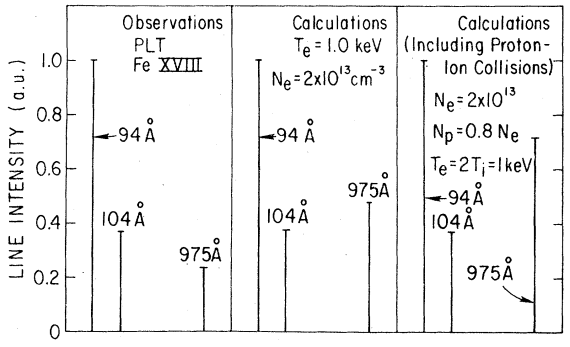

FIG. 5. Comparison of observed (a) relative intensities of Fe XVIII 94 Å, 104 Å, and forbidden line 975 Å with calculated intensities without (b) and with proton-iron collisions (c).

from level 1 ($2s^2 2p^5\ ^2P_{3/2}$) by electron and proton excitation, and from level 3 ($2s2p^6\ ^2S_{1/2}$) by electron collision and radiative deexcitation. Depopulation of level 2 was by radiative and collisional (electron and proton) deexcitation to level 1 and by electron collisional transition to level 3. Proton density in the calculations was assumed $N_p \approx 0.8\ N_e$ and the electron and ion temperatures at Fe XVIII emissivity maximum were 1.0 and 0.5 keV, respectively. Influence of higher levels was neglected as weakly coupled to level 2. The (extrapolated[33]) proton collisional excitation rate coefficient S_{12}^{p} for the $1 \rightarrow 2$ transition is comparable to the electron excitation rate coefficient,[30-33] for $T_i = 0.5$ keV and $T_e = 1.0$ keV. As a result, proton collisions should have a noticeable effect on the level 2 population for $N_p < 10^{14}/\text{cm}^3$, as shown in Fig. 4, although the level 3 population is not appreciably affected. However, comparing observed intensity ratios (Fig. 5) with the calculated values (for observed electron density) indicates that inclusion of the proton collisions makes the agreement worse. Quite similar effect was found in calculation of the 846 Å line of Fe XXII, where the relative electron and proton collisional rates are comparable to those of Fe XVIII. This probably indicates that the extrapolated proton rates (Appendix) are too high.

Calculations of Fe XX line intensities are presented in Fig. 6. Intensity of the 2665 Å line was calculated assuming that level $2s^2 2p^3\ 2D_{5/2}$ (level 3) is mainly excited by electron collisions from levels $2s^2 2p^3\ ^4S_{3/2}$ (level 1) and $2s^2 2p^3\ ^2D_{3/2}$ (level 2) and radiatively and collisionally deexcited to

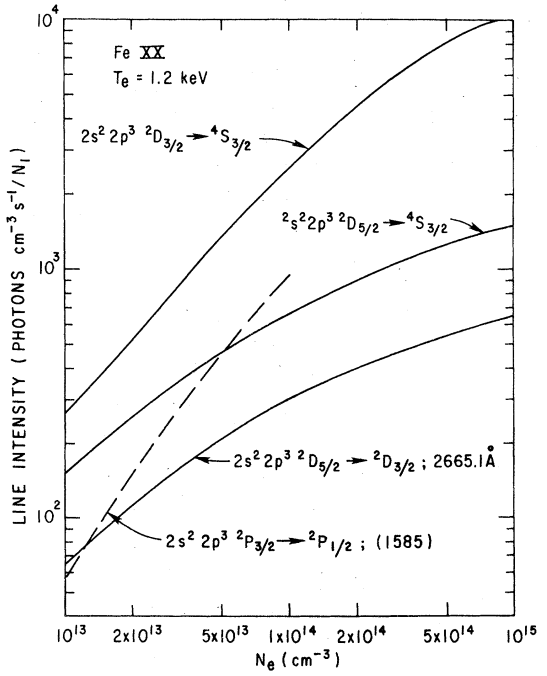

FIG. 6. Calculated intensities of selected Fe XX lines vs electron density. (Dashed curve from Feldman and Doschek calculations for 1585 Å line.)

levels 1 and 2. Population rate of level 3 from levels $2s^2 2p^3\ ^2P_{1/2,3/2}$ (levels 4 and 5) was small, and population from other levels was neglected. The calculated absolute value of the 2665 Å line is in good agreement with experiment,[1] i.e., the deduced Fe XX density is consistent with other ion densities, established from resonance line intensities. In Fig. 6, calculated intensity of intercombination lines from $3 \rightarrow 1$ and $2 \rightarrow 1$ transitions, (wavelengths[35] have not yet been observed) are also shown. According to calculations by Feldman and Doschek[34] the intensity of the second forbidden line (dashed curve in Fig. 6) with predicted wavelength 1585 Å should be larger than the intensity of the 2665 Å line in tokamak conditions.

For the Fe XXII 846 Å forbidden line intensity calculations we had to calculate simultaneously the population of six levels. The upper level of 846 Å line, $2s^2 2p\ ^2P_{3/2}$ (level 2) is directly populated from level $2s^2 2p\ ^2P_{1/2}$ (level 1) and from the levels of $2s2p^2$ configuration, $^2D_{3/2}$ (level 3), $^2D_{5/2}$ (level 4), $^2S_{1/2}$ (level 5), and $^2P_{1/2,3/2}$ (levels 6 and 7). Influence of levels $^4P_{1/2,3/2,5/2}$ (levels 8, 9, and 10, respectively) on level 2 population is small, so population of these levels was calculated independently of level 2 population calculations. In depopulation of level 2, besides radiative and collisional deexcitation to level 1 we included electron collisional transitions to levels 3–7.

All lines in Fig. 7 may be divided into three groups: (a) lines (populated strongly from level 2) with the fastest intensity changes versus electron density (156, 116, 114, and 101 Å), (b) those with nearly linear electron density dependence (136, 117, and 247 Å, populated almost entirely from level 1) and (c) the forbidden line (846 Å) with the slowest change of intensity. Therefore, the intensity ratio of lines from these different groups should be density dependent. Comparison of calculations with experiment[26] is shown in Fig. 8. Generally, the agreement of calculations with experiment is quite good except for the line 156 Å. This discrepancy for only one line suggests that perhaps the rate coefficient S_{24} for the 156 Å line from Ref. 31 should be higher or that the measured intensity is in fact superposition of the 156 Å line and some other unidentified line intensity. (Feldman[36] has suggested that a Cr XX resonance line may have sufficient intensity and required time dependence.)

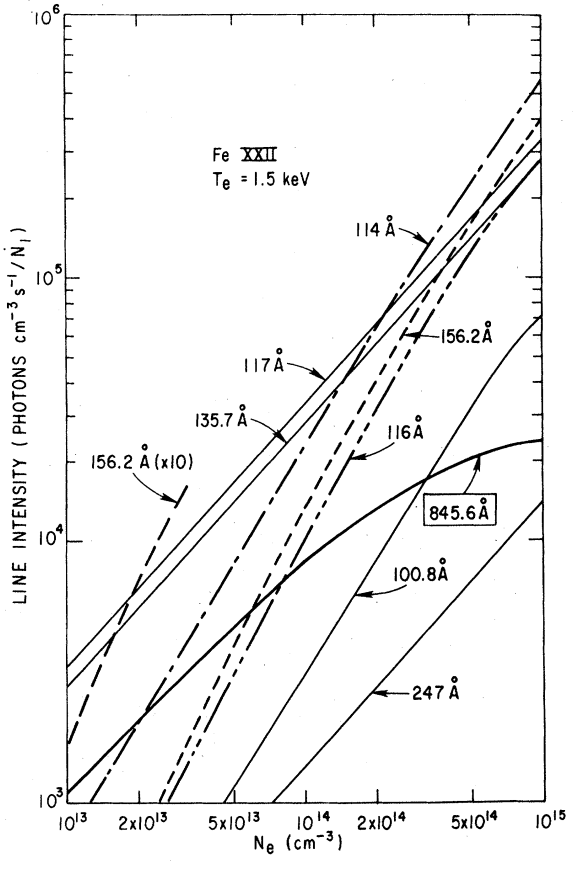

FIG. 7. Calculated intensities of selected Fe XXII lines vs electron density.

IV. CONCLUDING REMARKS

In typical PLT plasma in the spectral range 800–3000 Å forbidden lines of highly ionized iron

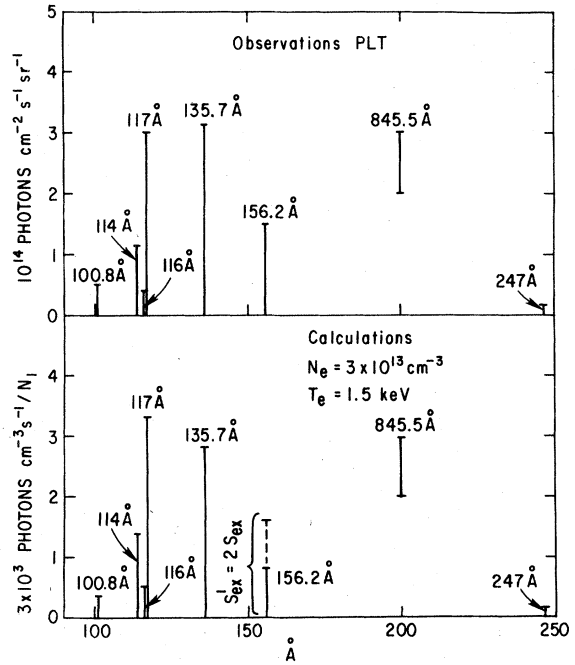

FIG. 8. Comparison of observed (a) and calculated (b) intensities of Fe XXII lines.

have intensity in the range 10^{13}–10^{14} photons $cm^{-2}\,sec^{-1}\,sr^{-1}$. These intensities are comparable with intensities of nonresonant lines from allowed transitions of the ions of the same stage of ionization. Influence of proton collisions on the forbidden line intensities is uncertain in the Ohmic heating discharges ($T_i < T_e$) but it may become quite significant during neutral-beam injection. The relatively high intensities, the high potentials of ionization of ions emitting such forbidden lines, and their long wavelengths, make these lines very important spectroscopy tools for high-temperature plasma diagnostics.

ACKNOWLEDGMENTS

The authors wish to thank our colleagues from the PLT and particularly K. Bol, R. J. Hawryluk, J. Hosea, E. Meservey, and J. Strachan for producing the discharges where the reported measurements were made, and N. Bretz, D. Dimock, and D. Johnson for providing us with information about electron density and temperature profiles. This work is supported by the United States Department of Energy, Contract No. EY-76-C-02-3073.

APPENDIX

In this Appendix we present the spontaneous transition probabilities A_{nm}, and the electron and proton excitation (S_{mn},S^p_{mn}) and deexcitation (S_{nm},S^p_{nm}) rate coefficients used for intensity calculations of Fe XVIII, Fe XX, and Fe XXII lines.

Fe XVIII

Approximate temperature of maximum density location in the plasma of the Fe XVIII, $T_e(\text{ion}_{max}) \approx 1.0$ keV ($T_i \approx 0.5$ keV)

λ (Å)	$n \rightarrow m$	A_{nm} (sec^{-1})	S_{mn}	S_{nm}	S^p_{mn}	S^p_{nm}
975	2 → 1	1.9(+4)[a]	1.8(−11)	3.6(−11)	≈8(−11)?	≈1.6(−10)?
94	3 → 1	9.5(+10)	1.6(−10)	3.2(−10)		
104	3 → 2	3.6(+10)	6.0(−11)	6.0(−11)		

Fe XX

$T_e(\text{ion}_{max}) \approx 1.2$ keV

λ (Å)	$n \rightarrow m$	A_{nm} (sec^{-1})	S_{mn}	S_{nm}
2665	3 → 2	5.7(+2)	3.7(−11)	2.6(−11)
≈630	3 → 1	1.3(+3)	2.6(−11)	1.8(−11)
≈824	2 → 1	1.6(+4)	1.8(−11)	1.8(−11)
1585	5 → 4	1.6(+3)		

Fe XXII

$T_e(\text{ion}_{max}) \approx 1.5$ keV ($T_i \approx 0.8$ keV)

λ (Å)	$n \rightarrow m$	A_{nm} (sec^{-1})	S_{mn}	S_{nm}	S^p_{mn}	S^p_{nm}
846	2 → 1	1.5(+4)	2.6(−11)	1.3(−11)	1.5(−10)?	8(−11)?
135.7	3 → 1	1.2(+10)	3.5(−10)	1.8(−10)		
156	4 → 2	6.4(+9)	2.5(−10)	1.7(−10)		
117	5 → 1	4.1(+10)	3.6(−10)	3.6(−10)		
135.9	5 → 2	4(+7)?	2.6(−12)	5.2(−12)		
102	6 → 1	2.4(+9)	1.2(−11)	1.2(−11)		
116	6 → 2	3.7(+10)	1.8(−10)	3.6(−10)		
100.8	7 → 1	6.4(+9)	7.5(−11)	3.8(−10)		
114	7 → 2	4.7(+10)	3.5(−10)	3.5(−10)		
247	8 → 1	9.7(+7)	1.6(−11)	1.6(−11)		

[a]Read 1.9(+4) = 1.9×10^4.

[1]S. Suckewer and E. Hinnov, Phys. Rev. Lett. 41, 756 (1978).
[2]H. Eubank *et al.*, *Proceedings of the Seventh International Conference on Plasma Physics and Controlled Nuclear Fusion* (IAEA, Innsbruck, Austria, 1978).
[3]S. Suckewer and E. Hinnov, Bull. Amer. Phys. Soc. 23, 875 (1978).
[4]B. Edlén, Z. Astrophys. 22, 47 (1942).
[5]B. Edlén, Mem. Soc. R. Sci. Liege 9, 235 (1976).
[6]A. H. Gabriel *et al.*, Astrophys. J 169, 595 (1971).
[7]E. Hinnov, Workshop of Theoretical Aspects of Atomic Physics in CTR, ORNL, 1975 (unpublished).
[8]R. D. Cowan, Los Alamos Scientific Laboratory Report No. LA-6679-MS, 1977 (unpublished).
[9]G. A. Doschek and U. Feldman, J. Appl. Phys. 47, 3083 (1976).
[10]G. D. Sandlin, G. E. Brueckner, and R. Tousey, Astrophys. J. 214, 898 (1977).
[11]A. H. Gabriel and C. Jordan, Mon. Not. R. Astron. Soc. 173, 397 (1975).
[12]H. Nussbaumer, Astrophys. J. 166, 411 (1971).
[13]S. Suckewer, Phys. Lett. 25A, 284 (1967); Phys. Rev. 170, 239 (1968).
[14]U. Feldman and G. A. Doschek, J. Opt. Soc. Am. 67, 726 (1977).
[15]D. Grove *et al.*, *Proceedings of the Sixth International Conference on Plasma Physics and Controlled Nuclear Fusion* (IAEA, Berchtesgarden, W. Germany, 1976).
[16]K. Bol *et al.*, *Proceedings of the Seventh International Conference of Plasma Physics and Controlled Nuclear Fusion* (IAEA, Innsbruck, Austria, 1978).
[17]E. Hinnov, Phys. Rev. A 14, 1533 (1976).
[18]E. Hinnov, S. Suckewer, K. Bol, R. J. Hawryluk, J. Hosea, and E. Meservey, Plasma Phys. 20, 723 (1978).
[19]S. Suckewer, E. Hinnov, and J. Schivell, PPPL Report 1430, Princeton, N. J., 1978 (unpublished).
[20]G. A. Doschek *et al.*, Astrophys. J. 196, L83 (1975).
[21]B. Edlén, Solar Phys. 24, 356 (1972).
[22]A. W. Weiss, J. Quant. Spectrosc. Radiat. Transfer 18, 481 (1977); also (private communication).
[23]S. O. Kastner, A. K. Bhatia, and L. Cohen, Physica Scr. 15, 259 (1977).
[24]J. Reader and J. Sugar, J. Phys. Chem. Ref. Data 4, 353–440 (1975).
[25]K. Mori, M. Otsuka, and T. Kato, *Grotian Diagrams of Highly Ionized Iron FeVIII-FeXXVI* (Nagoya University, Nagoya, 1977).
[26]E. Hinnov, Astrop. J. Lett. 230, L1 (1979).
[27]E. Hinnov *et al.*, Bull. Am. Phys. Soc. 23, 874 (1978).
[28]C. Breton, C. deMichelis, M. Finkenthal, and M. Mattioli Report No. EUR-CEA-FC-948, Fontenay-aux-Roses, France, 1978 (unpublished).
[29]C. Jordan, Mon. Not. R. Astron. Soc. 148, 17 (1970).
[30]A. Merts *et al.*, Report at Workshop on Atomic Processes in Controlled Thermonuclear Research, LASL, 1978 (unpublished).
[31]D. Robb (unpublished).
[32]M. Blaha, Astrophys. J. 157, 473 (1969).
[33]O. Bely and P. Faucher, Astron. Astrophys. 6, 88 (1970).
[34]U. Feldman and G. A. Doschek (private communication).
[35]K. Widing, Astrophys. J. 222, 735 (1978).
[36]U. Feldman (private communication).
[37]E. Hinnov, *Diagnostic for Fusion Experiments*, in *Proceedings of the Course, Varenna, Italy, Sept. 1978*, edited by E. Sindoni and C. Wharton (Pergamon, Oxford, 1979).